

**Calhoun: The NPS Institutional Archive**  
**DSpace Repository**

---

Theses and Dissertations

1. Thesis and Dissertation Collection, all items

---

1995-03

## Pressure sensitive paint measurement on a rotor

Varner, Donald R.

Monterey, California. Naval Postgraduate School

---

<http://hdl.handle.net/10945/7552>

---

This publication is a work of the U.S. Government as defined in Title 17, United States Code, Section 101. Copyright protection is not available for this work in the United States.

*Downloaded from NPS Archive: Calhoun*



Calhoun is the Naval Postgraduate School's public access digital repository for research materials and institutional publications created by the NPS community. Calhoun is named for Professor of Mathematics Guy K. Calhoun, NPS's first appointed -- and published -- scholarly author.

**Dudley Knox Library / Naval Postgraduate School**  
**411 Dyer Road / 1 University Circle**  
**Monterey, California USA 93943**

<http://www.nps.edu/library>

**NAVAL POSTGRADUATE SCHOOL**  
**Monterey, California**



**THESIS**

**PRESSURE SENSITIVE PAINT  
MEASUREMENT ON A ROTOR**

by

Donald R. Varner

March 1995

Thesis Advisor:

Raymond P. Shreeve

Thesis  
V3273

Approved for public release; distribution is unlimited.

DUDLEY KNOX LIBRARY  
NAVAL POSTGRADUATE SCHOOL  
MONTEREY CA 93943-5101

REPORT DOCUMENTATION PAGE			Form Approved OMB No. 0704
Public reporting burden for this collection of information is estimated to average 1 hour per response, including the time for reviewing instruction, searching existing data sources, gathering and maintaining the data needed, and completing and reviewing the collection of information. Send comments regarding this burden estimate or any other aspect of this collection of information, including suggestions for reducing this burden, to Washington headquarters Services, Directorate for Information Operations and Reports, 1215 Jefferson Davis Highway, Suite 1204, Arlington, VA 22202-4302, and to the Office of Management and Budget, Paperwork Reduction Project (0704-0188) Washington DC 20503.			
1. AGENCY USE ONLY (Leave blank)	2. REPORT DATE March 1995	3. REPORT TYPE AND DATES COVERED Master's Thesis	
4. TITLE AND SUBTITLE PRESSURE SENSITIVE PAINT MEASUREMENT ON A ROTOR			5. FUNDING NUMBERS
6. AUTHOR(S) Varner, Donald Ralph			
7. PERFORMING ORGANIZATION NAME(S) AND ADDRESS(ES) Naval Postgraduate School Monterey CA 93943-5000			8. PERFORMING ORGANIZATION REPORT NUMBER
9. SPONSORING/MONITORING AGENCY NAME(S) AND ADDRESS(ES)			10. SPONSORING/MONITORING AGENCY REPORT NUMBER
11. SUPPLEMENTARY NOTES The views expressed in this thesis are those of the author and do not reflect the official policy or position of the Department of Defense or the U.S. Government.			
12a. DISTRIBUTION/AVAILABILITY STATEMENT Approved for public release; distribution is unlimited.			12b. DISTRIBUTION CODE
13. ABSTRACT (maximum 200 words)  Toward the development of a measurement system for transonic compressor rotors, the static pressure field over a high-speed test rotor was recorded using pressure sensitive paint (PSP) and an electronically-gated, intensified CCD video camera and frame-grabber. Semi-conductor digital logic circuits were developed to form a phase-locked image capture system which acquired ultra-high-speed, low-light-level gated images once per revolution (1/Rev). A monostable-pulse circuit was developed to sum more than 200 gated images over a one-second integration period to build a single image. Rotor speed was measured on an oscilloscope using the 1/Rev trigger-pulse. Also, a pressure vessel was constructed and used to calibrate the PSP over varying pressure and temperature ranges to yield qualitative image intensity versus pressure data. Finally, the static pressure field data over the rotor surface was measured and presented as a 256 grey-scale and color image.			
14. SUBJECT TERMS Pressure Sensitive Paint, PSP, Photoluminescence, Imaging, Luminescence, PrOEP, UV Illumination, Detection, Emission, CCD, Aerodynamics, Measurements			15. NUMBER OF PAGES 65
			16. PRICE CODE
17. SECURITY CLASSIFICATION OF REPORT Unclassified	18. SECURITY CLASSIFICATION OF THIS PAGE Unclassified	19. SECURITY CLASSIFICATION OF ABSTRACT Unclassified	20. LIMITATION OF ABSTRACT UL



Approved for public release, distribution is unlimited.

**PRESSURE SENSITIVE PAINT  
MEASUREMENT ON A ROTOR**

by

Donald R. Varner  
Lieutenant, United States Navy  
B.A.E., Auburn University, 1987

Submitted in partial fulfillment of the  
requirements for the degree of

**MASTER OF SCIENCE IN AERONAUTICAL ENGINEERING**

from the

**NAVAL POSTGRADUATE SCHOOL  
March 1995**

Author:

  
Donald R. Varner

Approved by:

  
Raymond P. Shreeve, Thesis Advisor

  
Garth V. Hobson, Second Reader

  
Daniel J. Collins, Chairman,  
Department of Aeronautics and Astronautics

Thesis  
V3273  
c.2

## ABSTRACT

Toward the development of a measurement system for transonic compressor rotors, the static pressure field over a high-speed test rotor was recorded using pressure sensitive paint (PSP) and an electronically-gated, intensified CCD video camera and frame-grabber. Semi-conductor digital logic circuits were developed to form a phase-locked image capture system which acquired ultra-high-speed, low-light-level gated images once per revolution (1/Rev). A monostable-pulse circuit was developed to sum more than 200 gated images over a one-second integration period to build a single image. Rotor speed was measured on an oscilloscope using the 1/Rev trigger-pulse. Also, a pressure vessel was constructed and used to calibrate the PSP over varying pressure and temperature ranges to yield qualitative image intensity versus pressure data. Finally, the static pressure field data over the rotor surface was measured and presented as a 256 grey-scale and color image.



## TABLE OF CONTENTS

I. INTRODUCTION .....	1
II. TRANSONIC ROTOR CONSIDERATIONS .....	3
A. RAPID DATA SAMPLING .....	3
B. LOW LIGHT ENVIRONMENT AND INTEGRATION .....	3
C. HIGH CENTRIFUGAL LOADING .....	4
D. PAINT THICKNESS AND SURFACE ROUGHNESS .....	5
E. A PRIORI PAINT CALIBRATION .....	5
III. DESCRIPTION OF THE EXPERIMENT .....	7
A. CONCEPT AND LAYOUT .....	7
B. ROTOR SETUP .....	7
1. Test Rotor .....	7
2. Drive Unit .....	8
3. Spin Chamber .....	8
C. PAINT AND CALIBRATION CHAMBER .....	8
1. Paint Application .....	8
2. Calibration Chamber .....	9
D. LIGHTING AND CAMERA SYSTEM .....	9
1. UV Lamp .....	9
2. CCD Camera .....	10
3. Camera Control Unit .....	10
E. PHASE-LOCKED IMAGING .....	11
1. Once Per Revolution Trigger .....	11
2. Wave-Shaper Circuit .....	11
3. Voltage Divider/Inverter Circuit .....	11
4. Monostable-Pulse Circuit .....	12
5. Control Gate Circuit .....	12
6. Wind-Off Triggering .....	13

F. IMAGING AND PROCESSING .....	13
1. Frame-grabber and Software .....	13
2. Wind-On / Wind-Off / Dark Current Processing .....	13
IV. RESULTS AND DISCUSSION .....	27
A. PRELIMINARY STEADY FLOW MEASUREMENTS .....	27
1. Setup and Procedure .....	27
2. Results .....	27
B. PHASE-LOCKED ROTOR MEASUREMENTS .....	28
1. Procedure .....	28
2. Results .....	28
C. DISCUSSION .....	29
V. CONCLUSIONS AND RECOMMENDATIONS .....	39
APPENDIX A. PSP CALIBRATION RESULTS .....	41
APPENDIX B. CIRCUIT DIAGRAMS AND SCHEMATICS .....	45
LIST OF REFERENCES .....	53
INITIAL DISTRIBUTION LIST .....	55

## I. INTRODUCTION

The design of modern transonic compressor rotors relies heavily upon computational fluid dynamic (CFD) codes [Ref. 1]. Although an extremely powerful and useful design tool, CFD methods must be validated with measurements made when the designs are tested. Non-intrusive laser-Doppler velocimetry (LDV) can be used to determine the velocity field in a rotor, while holographic interferometry, or holography can, in principle, provide both aerodynamic (density) and mechanical behavior [Ref. 2]. Neither method, however, measures the static pressure field induced by the airflow on the rotating rotor blade. For non-rotating aerodynamic validation, surface pressure is usually the first feature to be compared with CFD predictions. Pressure taps and pressure transducers provide the capability of measuring surface pressure on stationary model surfaces (though they can be very expensive and time consuming to install), but their use for rotor blade measurements is not usually feasible. In recent years, pressure sensitive paint (PSP) has been developed and applied successfully to obtain surface pressure distributions on stationary models [Ref. 3].

The goal of the present work was to develop the means to obtain PSP measurements of pressure on the blade surfaces of a newly designed high-speed rotor [Ref. 1]. As a preliminary PSP test-bed for a method to be applied later on the Naval Postgraduate School (NPS) transonic compressor, a 12-inch diameter, high-speed, 2-bladed disk rotor was constructed. The goals of the rotor design were to achieve a transonic tip speed and a steady relative airflow, and to produce a shock across the rotor surface; an event that would produce a large variation in the static pressure field. A photodiode/light-emitting diode (LED) combination was used to trigger a high-speed, electronically-gated, intensified CCD camera once per revolution (1/Rev) when the appropriate (painted) blade was in position. The camera gate speed was on the order of microseconds in order to 'freeze' the rotor motion. The amount of light detected by the camera during the selected 1/Rev gate period was so low that the image was literally not

seen. It was therefore necessary to design and construct a phase-locked system, consisting of semi-conductor digital logic circuits, that allowed the integration of multiple 1/Rev gated images on the camera imager array in order to accumulate an observable image. A frame-grabber board in a personal computer (PC) was used to capture the image. An intensity versus pressure calibration curve was established using a test chamber to enable the video image to be quantified.

Since no previous applications of PSP to record rotor surface pressure have been reported, details of the present application have been included in the present report. First, the following section discusses the considerations involved in obtaining high-speed rotor PSP measurements. Section III then describes the experiment which was designed to demonstrate such measurements. Section IV discusses the results and Section V contains conclusions and recommendations. Appendix A describes the PSP calibration results and Appendix B shows detailed circuit diagrams and schematics that form the phase-locked system.

## II. TRANSONIC ROTOR MEASUREMENT CONSIDERATIONS

In arriving at the experiment reported herein, the intended application of PSP on a test rotor operated in the transonic compressor test rig, introduced considerations which are discussed in the following paragraphs.

### A. RAPID DATA SAMPLING

The airflow through a first stage compressor rotor is a steady flow in the rotor frame of reference. That the surface pressure be steady was a necessary requirement for the collection of quantitative information using current PSP techniques. Another equally important requirement was that the painted surface be steadily illuminated by the light source (here, an ultraviolet (UV) lamp) and that the camera receiving the luminescent emissions from the paint be stationary in relation to the surface. A transonic compressor rotor, turning many thousands of revolutions per minute (rpm), was far from stationary relative to the UV lamp or the camera. Strobing the blades with illumination was not a viable solution as the response time of the PSP once illuminated was on the order of 0.1-1.0 milliseconds, with the maximum intensity being emitted after a 1-2 minute induction period of continuous light [Ref. 4]. Therefore, in order to circumvent the problem of the response of the paint, and yet to make the rotating blades appear stationary to the camera, an electronically-gated intensified CCD video camera, operated with continuous illumination, was the chosen approach. Table 1 shows the relationship between rotor travel and camera gate speed.

### B. LOW LIGHT ENVIRONMENT AND IMAGE INTEGRATION

Currently, gate speeds as low as 20 nanoseconds were achievable with electronically-gated intensified CCD cameras. However, for single exposures, a very large amount of light, entailing the use of more than two 1000-Watt quartz-tungsten halogen lamps to illuminate a PSP coated surface would be required. Since the luminous intensity varied inversely as the square of the distance from the source, the closer the lamp was

placed to the painted surface the more light the paint would see. Unfortunately, due to the arrangement of the experimental setup, the requirement not to disturb the flowfield to be measured, and the size of the UV lamp housing, there was a significant, unavoidable distance between the painted surface and the lamp. Single gated images were not adequate, due to the very low light levels received at high gate speeds, therefore, multiple gated images, summed over a predetermined integration period, were necessary to produce a usable image.

<b>Rotor</b>				
<b>Tip Velocity</b>	<b>1/60 sec</b>	<b>1 millisecc</b>	<b>1 microsec</b>	<b>20 nanosec</b>
<b>(ft/sec)</b>				
600	120	7.20	0.0072	0.000144
800	160	9.60	0.0096	0.000192
1000	200	12.00	0.0120	0.000240
1200	240	14.40	0.0144	0.000288
1400	280	16.80	0.0168	0.000336

**Table 1. Rotor Travel Versus Camera Gate Speed**

### **C. HIGH CENTRIFUGAL LOADING**

High centrifugal loading due to rotation is not only a key factor in the structural design of transonic rotors, but determines whether the shape of the spinning rotor will be distorted when compared with the non-rotating shape. In the application of PSP, the distortion of the painted surface from the "wind-off" (non-rotating) to the "wind-on" (rotating) condition must be accounted for during image processing. Distortion, due to the blade **untwist** of the transonic compressor rotor, was an important consideration in the intended application, but one that could be avoided in the first stage of development of the technique.

#### **D. PAINT THICKNESS AND SURFACE ROUGHNESS FACTORS**

The application of PSP to a surface is, at first sight, a non-intrusive measurement technique [Ref. 5]. However, if the layer of paint on a transonic rotor blade is applied too thick or the surface is not a smooth one, it has been shown that severe losses in aerodynamic performance can occur [Ref. 6]. The adherence of the paint to the blading at high rotational speeds was anticipated to be an issue to be resolved by experiment. However, the experience of Suder et al. [Ref. 6] suggests that the 'intrusive' effect of the paint layer is the more significant issue. Again, the issue could be avoided in the first stage of development of the technique.

#### **E. A PRIORI PAINT CALIBRATION**

A priori calibration of the PSP was required for the rotor application since pressure taps could not be provided in the rotor surface for an "in situ" calibration between pressure and intensity. In the transonic test rig application, it was thought to be possible to carry out an a priori calibration with the rotor in place by applying controlled static pressures to the duct without rotor rotation. This approach would leave both the illumination source and camera detection arrangements common with the "wind-on" arrangement. However, in order to examine the potential problems of having to remove the rotor for a priori calibration in a separate test chamber, and to facilitate a priori calibration of PSP on the rotor used in the present development, a small calibration chamber was manufactured.



### III. DESCRIPTION OF THE EXPERIMENT

#### A. CONCEPT AND LAYOUT

The test rotor with PSP applied, untested and with somewhat unknown aerodynamic characteristics, was enclosed in a well-ventilated spin chamber for safety reasons. Separately, an aluminum plate with the same PSP coating was calibrated in a calibration chamber, or pressure vessel, in order that quantitative data be derived. The image capture and processing system was made up of three main subsystems; the lighting and camera system, the phase-locked sampling system, and the imaging and processing system. The overall layout diagram is shown in Figure 1. Details of each system are described in the following paragraphs.

#### B. ROTOR SETUP

##### 1. Test Rotor

The high-speed, two-bladed disk rotor shown in Figure 2, was designed to provide a simple, low-risk, easily machined, test platform for PSP measurements. The airfoil-shaped blades were designed to have sharp leading edges for supersonic flow, but were subsequently given blunt leading edges for structural reasons. Figure 3 shows a close-up of a rotor blade with dimensions, and Figure 4 shows an angled perspective. The centrifugal force on the blade, leading to high bending stresses, was the main structural design consideration. A safety factor (SF) of 2.0, or twice the ultimate yield stress, was used for rotational speeds up to 30,000 rpm. This was the reason for blunting the very thin, sharp leading edges, which did not meet the SF constraint. The rotor was fitted with a rectangular key-way to provide torque transmission between the rotor and the drive shaft, which was also designed specifically for the present experiment. The drive shaft and rotor were mounted to a commercially-available high-speed router, which served as the drive unit.

## **2. Drive Unit**

The rotor drive unit was a Bosch high-speed plunge router capable of a rotational speed of 25,000 rpm (unloaded condition) with 3-1/2 horsepower (HP) of available power. The design speed of 20,000 rpm with an estimated requirement of 2 HP, would provide the required transonic tip velocity. For safety reasons, for both personnel and other equipment in the laboratory, the unobstructed ideal airflow desired was sacrificed to some extent by enclosing the rotor and drive unit in a spin chamber as shown in Figure 5.

## **3. Spin Chamber**

The spin chamber was constructed using a 1/8 inch thick section of steel pipe measuring 30-inches in length and 24-inches in outside diameter. The chamber was mounted to a stand and then bolted to a wall for added support. A 2-inch gap was left between the front cover plate and the front of the tube, and similarly between the wall and the back of the tube. These gaps were necessary to allow unimpeded airflow. As shown in Figure 6, two holes were cut into the face plate for the UV lamp and camera. The camera and UV lamp placement are shown in Figure 7. The large distance between the UV lamp, mounted along rotor centerline, and the rotor ensured that the entire rotor surface would be continuously illuminated. The camera was located directly above the UV lamp in order that the painted blade be seen in the 12 o'clock position.

# **C. PAINT AND CALIBRATION CHAMBER**

## **1. Paint Application**

The paint used in the present development was obtained from NASA Ames Research Center [Ref. 5]. The paint contained platinum octaethylporphyrin (PtOEP), which has a phosphorescence known to be quenched by oxygen [Ref. 7]. When illuminated with UV light, the detected intensity distribution from the paint, imaged by the CCD camera, varied inversely and proportionally with the partial pressure of the oxygen at the surface. The PtOEP was dissolved in a silicone matrix to form the PSP. The PSP was applied over a Krylon white glossy paint (#1501) background using a small standard

hobby airbrush. The paint pattern is shown schematically in Figure 8. The glossy white paint backing was to help increase the signal-to-noise ratio of the image by serving as a reflecting surface for emitted light from the PtOEP. Kavandi [Ref. 7] and Seivwright [Ref. 8] discuss in detail the theory of PSP and its application.

## **2. Calibration Chamber**

The calibration chamber, shown in Figures 9 and 10, was used to subject a test plate, painted as described above, to a range of controlled uniform air pressures at two controlled temperatures. The pressure was varied from 0.5 to 40.0 psia. A vacuum pump was used for air evacuation, while a 300 psia compressed-air source was used for pressurization. Temperature, known to have a large influence on PSP measurements [Refs. 7,9], was monitored using a thermocouple probe and was controlled at 53° F and 66° F using a water bath.

The glass viewing window into the chamber, measuring 6 inches in diameter and 1/2-inch thick, allowed the passage of the UV frequencies required for illumination. Plans to use Plexiglas® were abandoned when it was found that only certain grades of Plexiglas would pass the frequencies required to excite the PSP [Ref. 10], and the glass on-hand worked satisfactorily.

The test plate, a small 3 inch diameter aluminum plate, positioned 1 inch below the inside surface of the viewing window, was painted with a Krylon glossy white backing and PSP. The CCD camera and UV lamp were located approximately 12 inches from the aluminum plate. The center 17 x 17 (289) pixels of the plate image were used to generate the calibration data shown in Appendix A.

## **D. LIGHTING AND CAMERA SYSTEM**

### **1. UV Lamp**

The UV lamp was an Oriol 1000-Watt quartz tungsten-halogen lamp [Ref.11] with an F/0.7 lens, controlled by an Oriol lamp controller [Ref. 12]. The lamp, shown in Figure 11, was fitted with an Oriol blue-gel filter (#66228) and an Oriol interference filter (#57521) to provide illumination at 380 nm. The voltage on the lamp controller was

always set at 110 percent to ensure consistency in exposure and allow as high an illumination level as practical. As time between integrated images was about 1 minute, the lamp was turned off between images to prevent degradation of the paint. Since the lamp had a 4 second ramp-up time from turn-on, a conservative 10 second illumination period was allowed before each image was captured. This ensured that a steady light source at full lamp strength was used for every image.

## **2. CCD Camera**

A Xyion ISG-350, electronically-gated, intensified CCD video camera, was used [Ref. 13]. An Oriol interference filter (#53590) was installed to allow only reception of the 650 nm illumination frequency. The camera, shown in Figure 12, had selectable gate speeds from 1/30th of a second to 20 nanoseconds. The gated camera block diagram is shown in Figure 13, and a breakdown of the intensifier elements is shown in Figure 14. The camera was controlled by a Xyion CCU-01 video camera control unit which is shown in Figure 15 [Ref. 14].

## **3. Camera Control Unit**

The CCU-01, which controlled the camera through a 23-pin, multi-purpose cable, accepted TTL active-low external-trigger signals through a BNC connector, and was used in an "image-inhibit" mode. The 1/Rev signal was the external-trigger input. The image-inhibit mode delayed the image acquisition period, normally 1/30th sec (frame) or 1/60th sec (field) rate, for a specified time period. Through a BNC connector on the CCU-01, a +5-volt signal was used to control the duration of the image-inhibit time. The image-inhibit function allowed multiple, extremely-low-light images to be integrated on the imager array, in order to accumulate an observable intensity. However, image blooming occurred on the image array if the image-inhibit function was active for more than about 1 second. In order to provide the required signals to the CCU-01, and ensure that synchronous timing of the external-trigger signals and image-inhibit signal occurred, a series of digital-logic circuits were devised which, with the camera and control unit, constitute a phase-locked imaging system.

## **E. PHASE-LOCKED IMAGING**

The phase-locked imaging system required several circuits. These circuits are discussed separately in the following paragraphs.

### **1. Once per Revolution Trigger**

The 1/Rev trigger-pulse circuit consisted of a LED which illuminated a photodiode through a 1/32 inch diameter hole in the rotor. The hole, at a radius of 5 inches from the rotor center, as shown in Figure 2, was located such that when the photodiode was illuminated, the painted blade was at the 12 o'clock position. However, the +50 millivolt signal generated by the photodiode, as depicted in Figure 16(a), was too small and poorly shaped to use as a trigger-pulse for TTL circuits, which use 5-volt square waves. The signal was therefore amplified and shaped using a circuit, designed and previously used at NPS, called a wave-shaper [Ref. 15].

### **2. Wave-Shaper Circuit**

The wave-shaper circuit, powered by a 9-volt dc power supply, was used to amplify the +50 millivolt pulse to a 9-volt, active-low, square wave, as shown in Figure 16(b). The signal, too large for TTL circuits, was therefore modified using a voltage-divider/inverter circuit.

### **3. Voltage-Divider / Inverter Circuit**

The voltage divider/inverter circuit changed the 9-volt active-low signal into a 5-volt active-high TTL signal as shown in Figure 16(c). Also, the 9-volt power output from the wave-shaper was reduced to 5-volts through a voltage-divider in order to power a TTL logic-control gate circuit (discussed in Section E.5). The voltage-divider/inverter circuit diagram and schematic are shown in Figures B-1 and B-2, respectively, in Appendix B [Ref. 16].

#### 4. Monostable-Pulse Circuit

In order that the camera integrate multiple gated images on the imager array, a 1-second TTL active-high square wave was needed. Initiated by a single TTL active-high pulse from a Wavetek pulse generator (Figure 16(d)), the 1-second square wave was input to the *image-inhibit* BNC connector on the CCU-01 (Figure 16(e)). While the image-inhibit function was activated, all subsequent 1/Rev trigger-pulses, input to the *ext trigger* BNC on the CCU-01 which gated the camera, acted to build the image. To assure that the trigger-pulse to the frame-grabber "grabbed" only the built-up or integrated image, a slightly shorter duration image-inhibit signal was sent to the *ext in* (external input) BNC on the frame-grabber board in the PC. This slightly shorter variable TTL active-high pulse, as shown in Figure 16(f), was also generated by the monostable pulse circuit [Ref. 17]. Figures B-3 and B-4, in Appendix B, show the monostable-pulse circuit diagram and schematic. Since the 1/Rev TTL active-high signals were continuously being sent to the external-trigger input on the CCU-01, and only the trigger pulses during the monostable-pulse were desired, a TTL logic-control gate circuit was built [Ref. 18].

#### 5. Control Gate Circuit

The TTL logic-control gate was a 2-input, quad, nand gate. The circuit diagram and schematic are shown in Figures B-5 and B-6, respectively, in Appendix B. As Figure B-5 shows, when input *A* (the monostable-pulse) was high, and input *B* (the 1/Rev TTL active-high trigger) was alternated between low and high (as it triggered), the output was an alternating high and low trigger, or a TTL active-low trigger. The CCU-01 external-trigger input needed to be a TTL active-low trigger in order to gate the camera. Thus the control gate not only allowed the camera to 'see' the trigger only during the monostable-pulse or image-inhibit period, but it also allowed the camera to see the inverted or proper signal (Figure 16(g)).

## 6. Wind-Off Triggering

Wind-off triggering was accomplished using a Wavetek function generator. Since the rotor had to be stationary during the wind-off imaging, a signal of equal period and pulse-width was generated to simulate the 1/Rev signal from the rotor. The rotor blade was aligned to the 12 o'clock position, in exactly the same orientation as the captured wind-on image, in order that the ratioed images be aligned. This made it unnecessary to use image alignment and manipulation procedures during image processing.

## F. IMAGING AND PROCESSING

### 1. Frame-grabber and Software

An Epix 4MEG Video Model 12 frame-grabber board and Epix 4MIP Interactive Image Analysis software (version 2.8) comprised the image processing system. The video resolution for each image was 761 x 240 pixels, or 360,960 pixels per image. The board was configured for 11 images, but with the version 2.8 software, only 1 triggered image at a time was able to be captured [Ref. 19]. Each image was subsequently stored on floppy disk.

### 2. Wind-On / Wind-Off / Dark Current Processing

The processing of PSP images is based upon the relationship between pressure and intensity,

$$I_o/I = A (P/P_o) + B \quad (1)$$

which is a form of the Stern-Volmer relationship. The intensity 'seen' by the camera during the reference "wind-off" condition ( $I_o$ ) was ratioed with the "wind-on" condition (I). Ratioing accounted for, and systematically eliminated any inconsistencies in the paint on the rotor surface. The associated pressures corresponding to the wind-off and wind-on conditions are  $P_o$  and  $P$ , respectively, and  $A$  and  $B$  are constants such that  $A + B = 1$  (see Appendix A). Dark current from the camera was subtracted from the wind-off and wind-on images before ratioing [Ref. 7]. Dark current, although usually obtained with the

lens cap on the camera, was here obtained with the lens cap off, in laboratory 'darkness'. This process not only accounted for camera dark-current, but also accounted for any image "noise" the 660 nm LED produced.

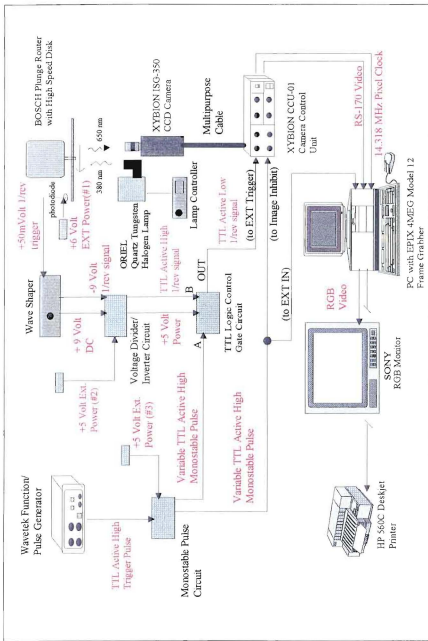
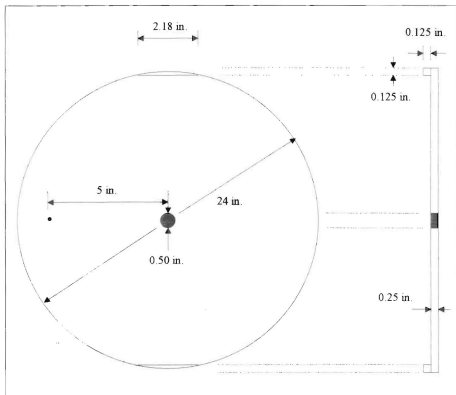
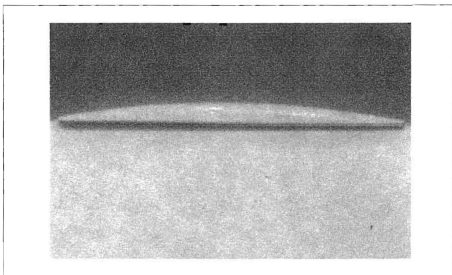


Figure 1. Rotor Equipment Setup and Signal Flow





**Figure 2. Test Rotor Dimensions**



**Figure 3. Rotor Blade Front View**



**Figure 4. Rotor Blade Angled View**

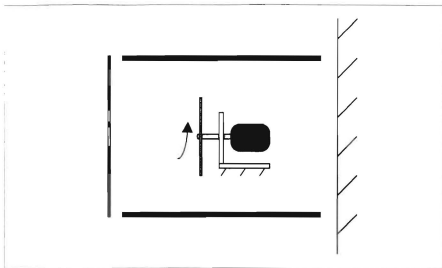


**Figure 5. Spin Chamber Setup**

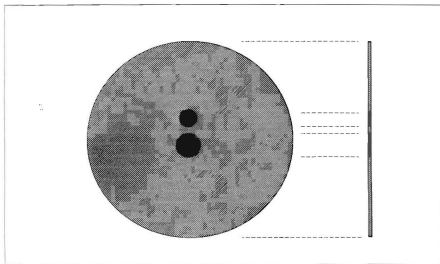


**Figure 6. Spin Chamber Face Plate**

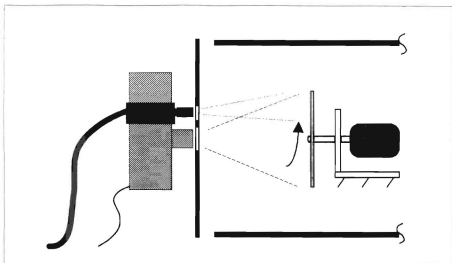


**Figure 7. Camera and Lamp Placement**



**Figure 8. Paint Distribution Over Rotor**

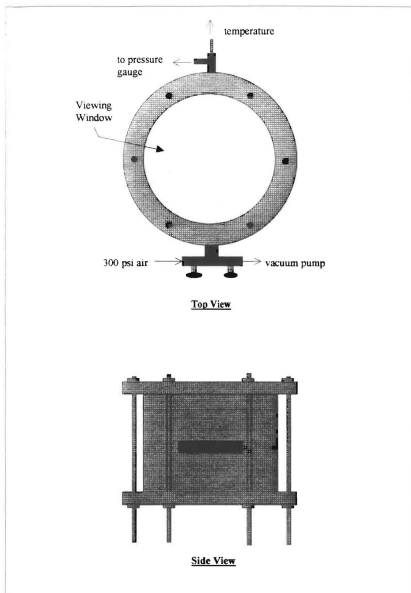


**Figure 9. Calibration Chamber**

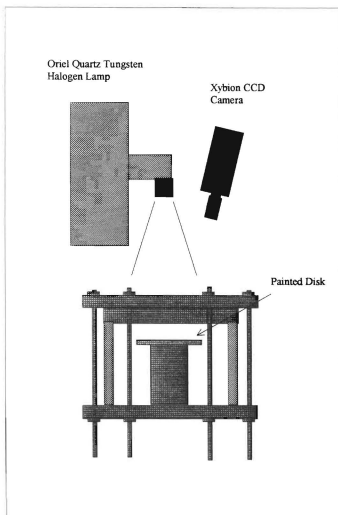


**Figure 10. PSP Calibration Setup**

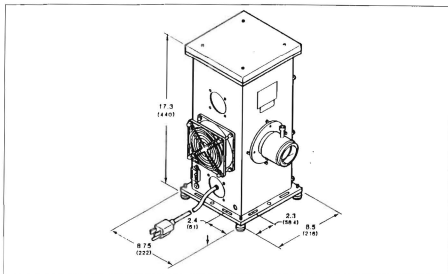


Figure 11. Oriel Quartz Tungsten Halogen Lamp [From Ref. 11]

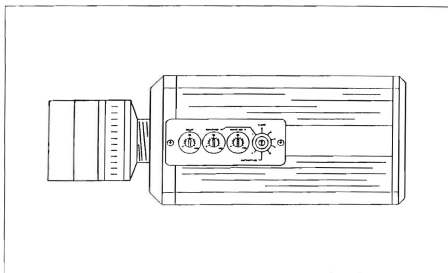


Figure 12. Xybion Electronically Gated Intensified CCD Video Camera [From Ref.13]

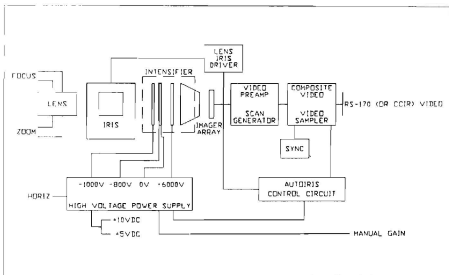


Figure 13. Camera Gate Block Diagram [From Ref. 13]

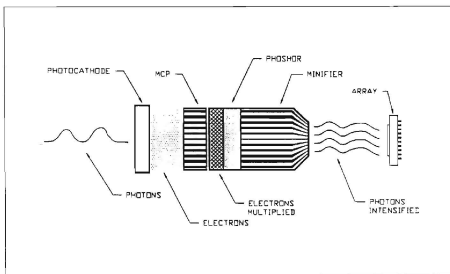


Figure 14. Camera Intensifier Elements [From Ref. 13]





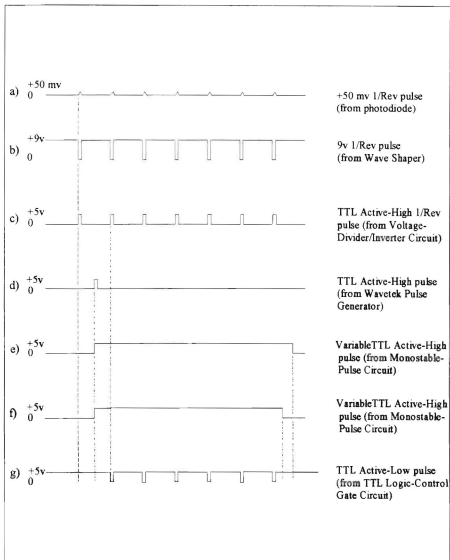


Figure 16. Image Capture Signal Flow Sequence



## IV. RESULTS AND DISCUSSION

### A. PRELIMINARY STEADY-FLOW MEASUREMENTS

As a procedural "stepping-stone" toward obtaining PSP measurements on a rotor, a preliminary, steady-flow experiment was performed using an under-expanded free-jet on a PSP coated, flat-plate surface. The experiment, previously and successfully performed by Seivwright [Ref. 8] with a Cohu 4910 Series CCD camera, was repeated with a Xybion ISG-350 CCD camera.

#### 1. Setup and Procedure

The experimental setup, similar to Seivwright's as shown in Figure 17, allowed measurement of static pressure on the flat-plate surface using 12 pressure taps (Figure 18). PSP was applied to the plate and a 65 psia (plenum pressure), under-expanded free-jet, was blown over the plate surface. The Xybion camera detected the luminescent intensity emitted by the paint. One-hundred wind-on, wind-off, and dark-current images were recorded using an Epix frame-grabber board and image processing software.

#### 2. Results

The 100 wind-on ( $I$ ), wind-off ( $I_0$ ) and dark-current images were averaged, respectively, and the dark-current average was subtracted from the averaged  $I$  and  $I_0$  images. The averaged  $I_0$  and  $I$  images were then ratioed ( $I/I_0$ ) to yield a 256 gray-scale image. Using the software's colorization routine, a color image was produced. Figure 19 shows the image (the direction of flow was from the left of the figure to the right). The intensity distribution, which varied inversely with pressure, was illustrated with a color distribution from red (lowest intensity) to dark-blue (highest intensity). The structure of the flow field shown in Figure 19, was investigated by and is reported by Seivwright [Ref. 8]. The surface pressure distribution obtained concurrently from static pressure tap measurements is shown in Figure 20. With qualitative agreement observed in these results, effort was directed at obtaining results from the rotor.

## B. PHASE-LOCKED ROTOR MEASUREMENTS

### 1. Procedure

The 12-inch rotor, painted as shown in Figure 8, was enclosed in the spin-chamber and rotated at maximum router power. The maximum speed attained at the rim gave Mach number = 0.63 at a rotational-speed of 13,300 rpm. The tip-speed was 696.38 ft/sec and the time for one revolution was 4.5 milliseconds, or 12.53  $\mu$ sec per degree of rotor travel. It was found experimentally that, with the 1000-Watt Oriel UV lamp and the Xybion camera, a minimum of 400  $\mu$ sec of total illumination time was necessary to "see" an image. (In 400  $\mu$ sec, the rotor would have turned approximately 32 degrees, yielding an impossibly blurred image.) It was therefore necessary to "build" the 1-second integrated image from 221 gated-images (from the 1/Rev trigger) at gate-speeds of 1.8  $\mu$ sec. The amount of rotor-tip rotation during 1.8  $\mu$ sec's was 0.14 degrees, or 0.0146 inches, which was small enough to prevent detectable image blur. Eighty integrated wind-on, wind-off and dark-current images were taken in the phase-locked mode, averaged, and ratioed.

### 2. Results

Histograms showing the frequency (no. of pixels) versus  $I_0$ ,  $I$ , and  $I/I$  (multiplied by a factor of 70) for tip Mach number = 0.63 is shown in Figure 21. Dark-current, shown in Figure 22, was subtracted from the  $I$  and  $I_0$  images before calculating the ratio. The computed values of  $I/I$  spanned a decimal range from 1.6 to 2.8 (Figure 23). To form the "ratioed image", these decimal values were multiplied (within the software) by a factor of 70 before reconversion to integer (Figure 24). The factor of 70, by trial-and-error, yielded the best spread of data over the 0 to 255 (gray-scale) range. The result of colorizing the ratioed image is shown in Figure 25.

### C. DISCUSSION

The results in Figure 25, show an intensity distribution that was clearly not uniform. The intensity distribution, from red (lowest intensity) near the disk center, to dark blue (highest intensity) at the rotor tip, suggested that pressure, inversely proportional to intensity, decreased in going from the rotor center toward the tip.

As shown in Figure 26 (from Ref. 20), the rotating disk will create a viscous pumping effect in which air will be sucked in along the axis and pumped out at the rim. While the radial pressure variation to be expected in the present apparatus as a result of this effect is not readily calculated, it is likely that a stagnation effect on the radial pumping would be created by the blades at the rim. Thus the area of yellow and red along the inner surface of the blade in Figure 25 may be qualitatively explained.

A first attempt to quantify the pressure distribution shown in Figure 25, using the calibration performed on a 'similar' sample in the calibration chamber, was not successful. As can be seen in Figure A-2, the values obtained for  $I_r/I$  from the rotor were well out of the range of values obtained in the calibration. If the calibration obtained on the sample in the chamber applied to the paint on the rotor, pressures of 3 to 6 atmospheres were experienced on the rotor. This clearly was not possible. A perfect (frictionless) impeller could pump to an increase in pressure no greater than 0.65 atmospheres. Therefore, while the qualitative variations seen in Figure 25 may be correct, the magnitudes of  $I_r/I$  obtained in the rotor experiment are suspect. It is unlikely that the unknown temperature of the paint on the rotor would provide the explanation since the discrepancy is too large. A more probable explanation involves the differences in the trigger signals used in the wind-off and wind-on imaging. While no error is known to have occurred in the procedure that was followed, a careful interrogation of the procedure is recommended as the next step.



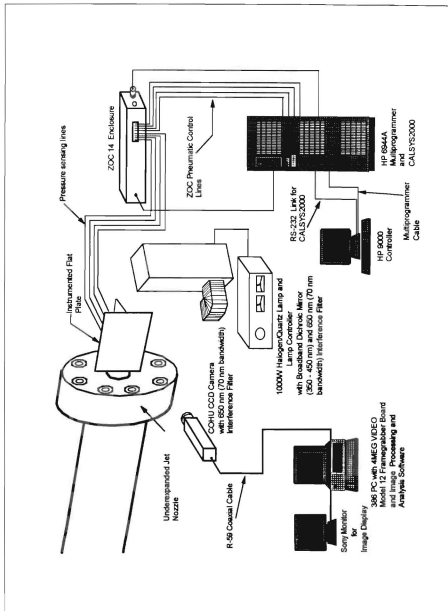


Figure 17. Underexpanded Free-Jet Set-Up [From Ref. 8]

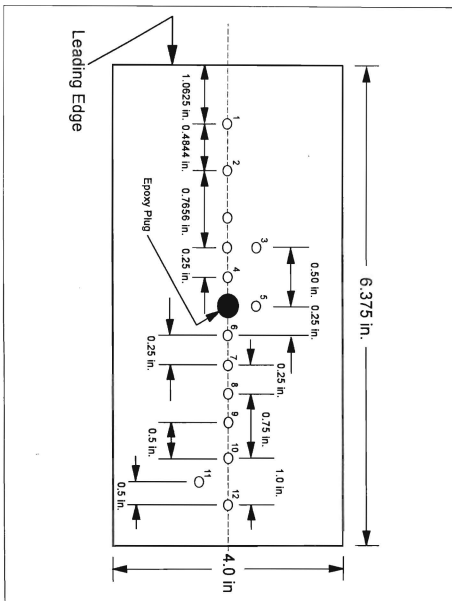


Figure 18. Flat-Plate Schematic [From Ref. 8]

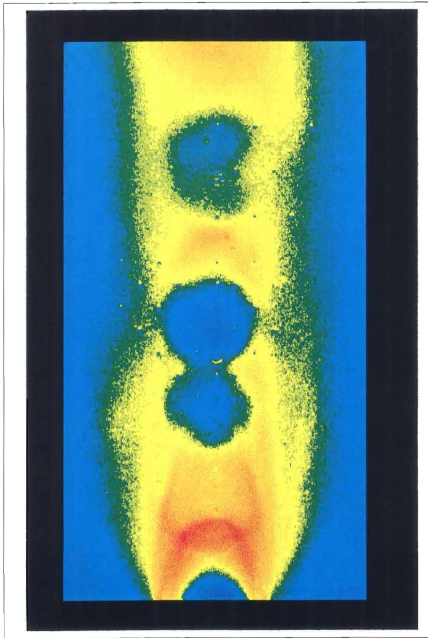


Figure 19. Underexpanded Freejet Over a Flat-Plate (65 PSIA Plenum Pressure)



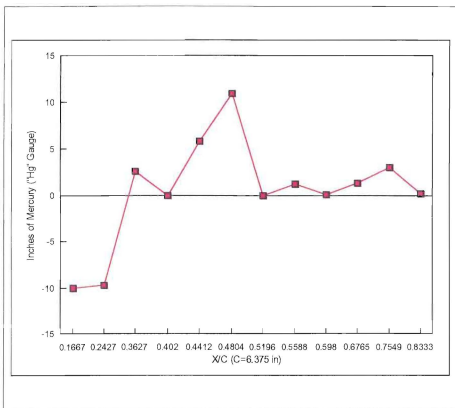


Figure 20. Pressure Distribution Over Flat-Plate (65 psig Plenum Pressure)



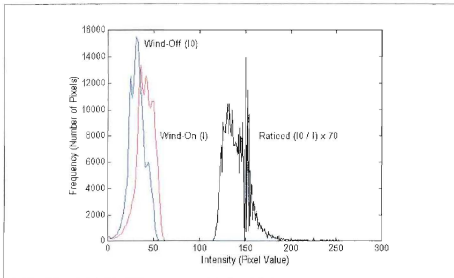


Figure 21. Rotor Pixel Frequency Versus Intensity

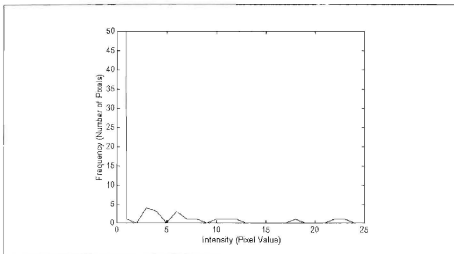
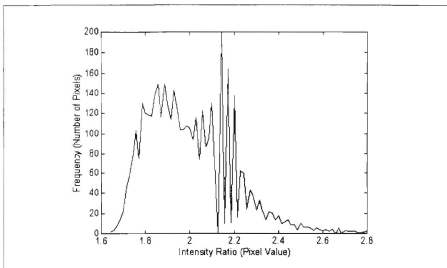
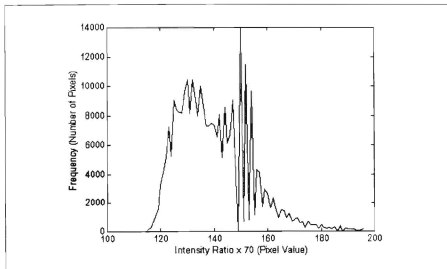


Figure 22. Dark-Current Pixel Frequency Versus Intensity

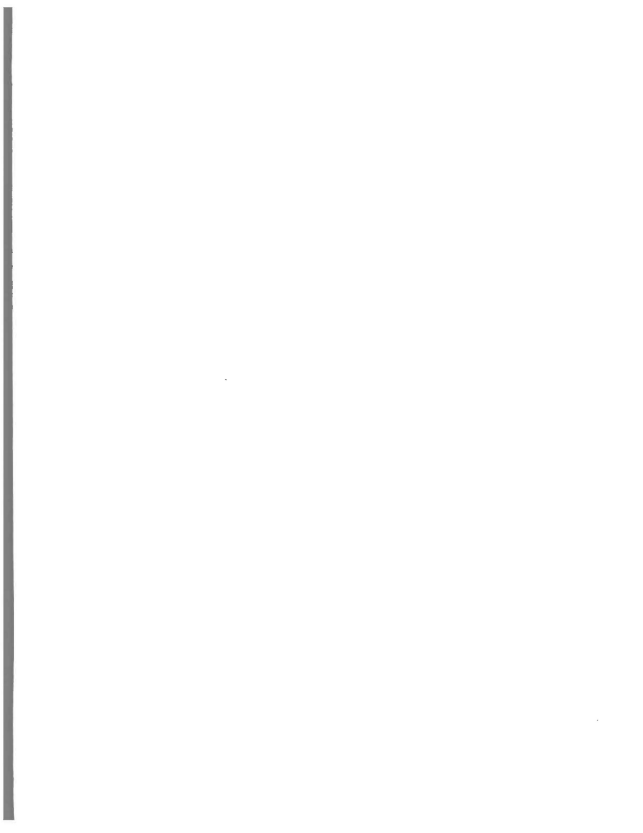




**Figure 23. Rotor Pixel Frequency Versus Intensity Ratio ( $I_r/I$ )**



**Figure 24. Rotor Pixel Frequency Versus Intensity Ratio ( $I_r/I \times 70$ )**



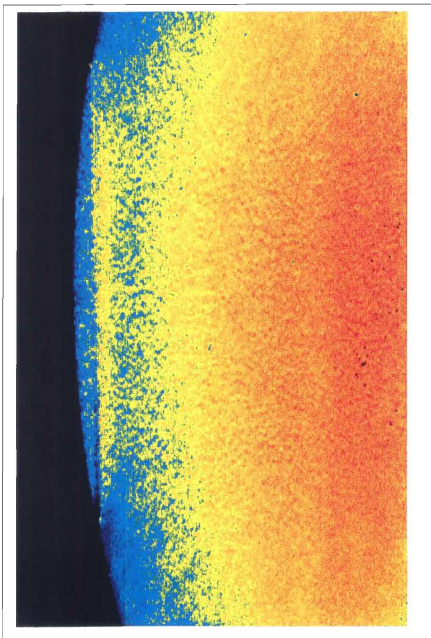


Figure 25. PSP Image of a 2-Bladed Disk Rotor



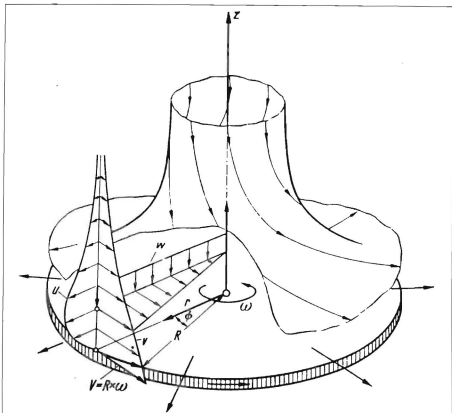


Figure 26. Velocity Flow-Field Over a Rotating Disk [From Ref. 20]



## V. CONCLUSIONS AND RECOMMENDATIONS

Phase-locked imaging, using pressure sensitive paint to obtain the surface-pressure distribution on a high-speed rotor, has been demonstrated successfully. While quantitative results were not obtained, pressure variations were recorded with well-focused images. Interpretation of the observed pressure variations was difficult because the rotor could not be operated at the supersonic rim speeds necessary to generate the intended shock wave over the surface. Considerably more than three horsepower was found to be required to drive the test rotor to sonic speeds. The test rotor itself was shown to be a useful design for the purpose of developing the phase-locked imaging technique.

To continue the development of a phase-locked imaging PSP system for transonic rotors, the following are recommended:

1. Critically examine the number of images and integration times during wind-on and wind-off imaging. The one-second integration time used was calculated to allow about 221 gated-images to build the image on the imager array. In order to know exactly how many trigger-pulses were used during the integration cycle, a simple 3-digit BCD counter-circuit (shown in Ref. 18) should be incorporated. The number of pulses used during the wind-on cycle can be recorded, and the Wavetek can be shown to provide the same number of pulses for the wind-off cycle.
2. Increase the drive power to obtain sonic wheel speeds.
3. Measure temperature within the chamber during operation and of the disk immediately on shut-down.
4. Obtain credible results and experience with the test rotor prior to installation on the transonic-compressor test-rig.



## APPENDIX A. PSP CALIBRATION RESULTS

PSP calibration-chamber results are shown in Figure A-1 for controlled pressures from 0.5 to 40 psia, at two controlled temperatures, 53 and 66 degrees F, respectively. The relationships between pressure and intensity, in the usual Stern-Volmer form, for the two temperatures were derived (by curve-fitting) as

$$I_p/I = 0.352 (P/P_0) + 0.679 \quad [66 F] \quad (A-1)$$

and

$$I_p/I = 0.353 (P/P_0) + 0.678 \quad [53 F] \quad (A-2)$$

Using equation (A-1) to extend the range as shown in Figure A-2, the  $I_p/I$  experimental data obtained from the test rotor gave  $P/P_0$  values larger than 6.



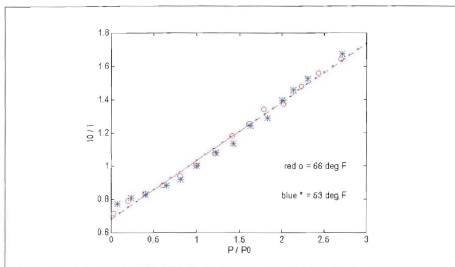


Figure A-1. PSP Calibration Curve

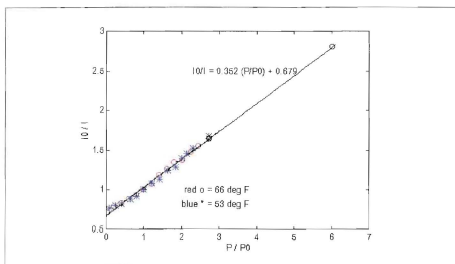


Figure A-2. Extended PSP Calibration Curve







## APPENDIX B. CIRCUIT DIAGRAMS AND SCHEMATICS



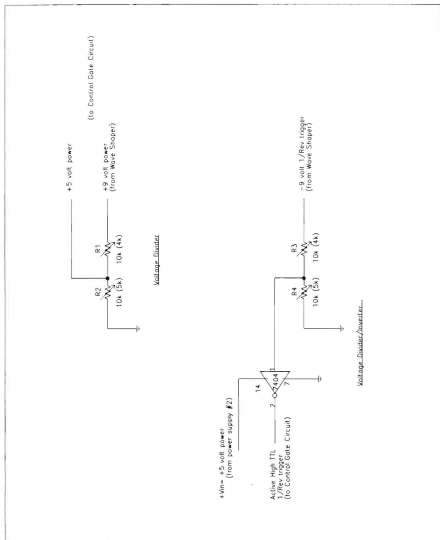


**Figure B-1. Voltage-Divider/Inverter Circuit Diagram**

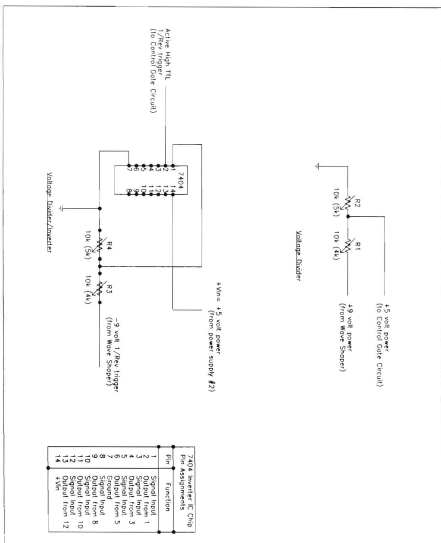


Figure B-2. Voltage-Divider/Inverter Circuit Schematic

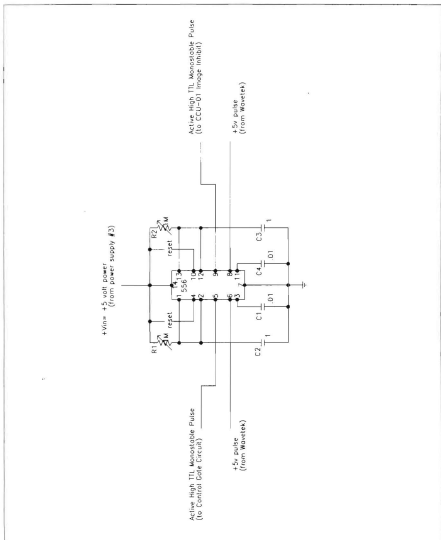


Figure B-3. Monostable-Pulse Circuit Diagram

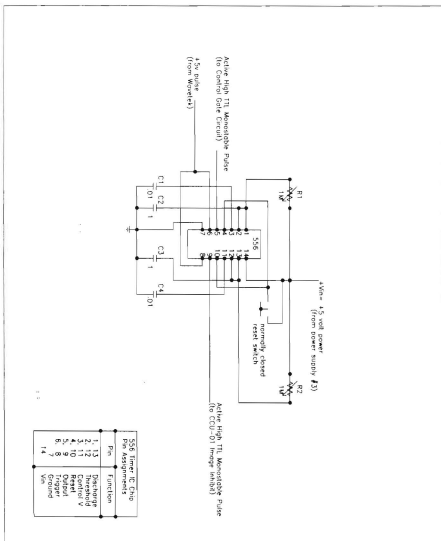
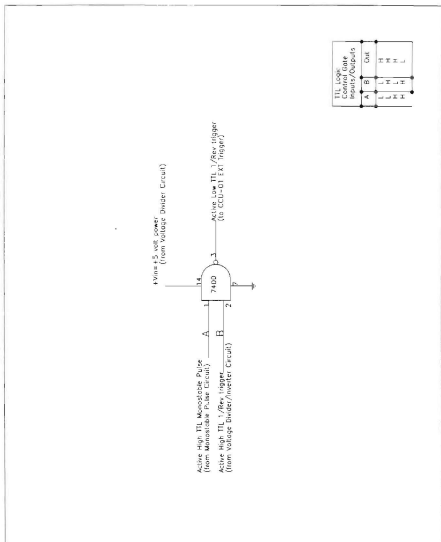


Figure B-4. Monostable-Pulse Circuit Schematic



**Figure B-5. TTL Logic-Control Gate Circuit Diagram**

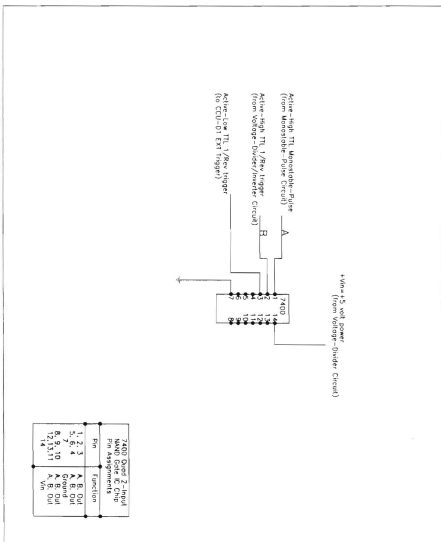


Figure B-6. TTL Logic-Control Gate Circuit Schematic

## LIST OF REFERENCES

1. Sanger, N. L., "Design of a Low Aspect Ratio Transonic Compressor Stage Using CFD Techniques," ASME Paper No. 94-GT-236, Presented at the International Gas Turbine and Aeroengine Congress and Exposition, The Hague, The Netherlands, June 13-16, 1994.
2. Parker, R. J., and Jones, D. G., "The Use of Holographic Interferometry for Turbomachinery Fan Evaluation During Rotating Tests," ASME *Journal of Turbomachinery*, vol. 110, July 1988.
3. Kavandi, J., Callis, J., Gouterman, M., Khalil, G., Wright, D., Green, E., Burns, D., McLachlan, B., "Luminescent Barometry in Wind Tunnels," *Rev. Sci. Instrum.*, Vol. 61, No. 11, 1991.
4. Uibel, R., Khalil, G., Gouterman, M., Gallery, J., and Callis, J., "Video Luminescent Barometry: The Induction Period," AIAA Paper No. 93-0179, 31st Aerospace Sciences Meeting & Exhibit, Reno, Nevada, January 11-14, 1993.
5. McLachlan, B. G., Kavandi, J. L., Callis, J. B., Gouterman, M., Green, E., Khalil, G., and Burns, D., "Surface Pressure Field Mapping Using Luminescent Coatings," *Experiments in Fluids*, Vol. 14, 1993.
6. Suder, K. L., Chima, R. V., Strazisar, A. J., and Roberts, W. B., "The Effect of Adding Roughness and Thickness to a Transonic Axial Compressor Rotor," ASME Paper No. 94-GT-339, Presented at the International Gas Turbine and Aeroengine Congress and Exposition, The Hague, The Netherlands, June 13-16, 1994.
7. Kavandi, J. L., "Luminescence Imaging for Aerodynamic Pressure Measurements," Ph.D. Dissertation, Department of Chemistry, University of Washington, 1990.
8. Seivwright, D. L., "Application of Pressure Sensitive Paint in Shock Boundary Layer Interaction Experiments," M.S. Thesis, Naval Postgraduate School, March 1995.
9. Donovan, J. F., Morris, M. J., Pal, A., Benne, M. E., Crites, R. C., "Data Analysis Techniques for Pressure- and Temperature-Sensitive Paint," AIAA Paper No. 93-0179, 31st Aerospace Sciences Meeting & Exhibit, Reno, Nevada, January 11-14, 1993.
10. Plexiglas® Acrylic Sheet, General Information and Physical Properties, Fax Memo from Rich West of Laird Plastics, March 1995.

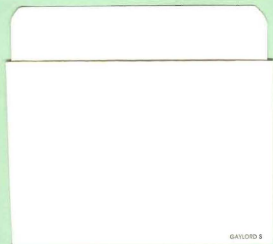
11. Oriel Instruction Manual, "Quartz Tungsten Halogen Lamp Housings," Models 66186 Through 66188, 1993.
12. Oriel Instruction Manual, "Lamp Controller," Model 6405, 1992.
13. Xybion Electronic Systems User's Manual, "Electronically Gated Intensified CCD Video Camera," Model ISG-350, May 1992.
14. Xybion Electronic Systems User's Manual, "Video Camera Control Unit," Model CCU-01, September 1990.
15. West, J. C., "Digital Programmable Timing Device for Fast Response Instrumentation in Rotating Machines," M.S. Thesis, Naval Postgraduate School, June 1976.
16. Mims, F. M., III, *Engineer's Mini-Notebook: Basic Semiconductor Circuits*, Radio Shack Cat No. 276-5013A, p. 8, Siliconcepts, 1993.
17. Mims, F. M., III, *Engineer's Mini-Notebook: 555 Timer IC Circuits*, Radio Shack Cat No. 276-5010A, p. 6, Siliconcepts, 1993.
18. Mims, F. M., III, *Engineer's Mini-Notebook: Digital Logic Circuits*, Radio Shack Cat No. 276-5014A, p. 16, Siliconcepts, 1993.
19. Epix User's Manual, "4MIP-4MIPTOOL Interactive Image Analysis," Version 2.8, 1993.
20. Schlichting, H., *Boundary Layer Theory*, p. 102, McGraw-Hill, 1979.

## INITIAL DISTRIBUTION LIST

1. Defense Technical Information Center..... 2  
Cameron Station  
Alexandria, VA 22304-6145
2. Dudley Knox Library..... 2  
Code 052  
Naval Postgraduate School  
Monterey, CA 93943-5101
3. Chairman..... 1  
Department of Aeronautics and Astronautics  
Code AA  
Naval Postgraduate School  
699 Dyer Road - Room 137  
Monterey, CA 93943-5106
4. Professor R. P. Shreeve..... 10  
Department of Aeronautics and Astronautics  
Code AA/SF  
Naval Postgraduate School  
699 Dyer Road - Room 137  
Monterey, CA 93943-5106
5. Professor G. V. Hobson..... 1  
Department of Aeronautics and Astronautics  
Code AA/Hg  
Naval Postgraduate School  
699 Dyer Road - Room 137  
Monterey, CA 93943-5106
6. Curricular Officer, Code 31..... 1  
Naval Postgraduate School  
Monterey, CA 93943-5002

7. Commander.....	1
Naval Air Systems Command	
Code Air 4.4.T	
1421 Jefferson Davis Hwy.	
Arlington, VA 22243	
8. Naval Air Warfare Center - Aircraft Division.....	1
Code Air - 4.4.3.1 [S. McAdams]	
Propulsion and Power Engineering, Bldg. 106	
Patuxent River, MD 20670-5304	
9. CWO3 Donald C. Varner.....	3
4228 Sandy Bluff Drive	
Gulf Breeze, FL 32561	
10. Lt. Donald R. Varner.....	2
Fleet Air Keflavik	
PSC 1003, Box 2	
FPO AE 09728-0302	

DUDLEY KNOX LIBRARY  
NAVAL POSTGRADUATE SCHOOL  
MONTEREY CA 93943-5101



GAYLORD 5

DUDLEY KNOX LIBRARY



3 2768 00311174 1